CHEMISTRY
A European Journal

A Journal of
ChemPubSoc Europe

Accepted Article

Title: The Chiral Twist-Bend Nematic Phase (N*TB)

Authors: Rebecca Walker, Damian Pociecha, John Mervyn David Storey, Ewa Gorecka, and Corrie Thomas Imrie

This manuscript has been accepted after peer review and appears as an Accepted Article online prior to editing, proofing, and formal publication of the final Version of Record (VoR). This work is currently citable by using the Digital Object Identifier (DOI) given below. The VoR will be published online in Early View as soon as possible and may be different to this Accepted Article as a result of editing. Readers should obtain the VoR from the journal website shown below when it is published to ensure accuracy of information. The authors are responsible for the content of this Accepted Article.

To be cited as: *Chem. Eur. J.* 10.1002/chem.201903014

Link to VoR: http://dx.doi.org/10.1002/chem.201903014

Supported by
ACES

WILEY-VCH

10.1002/chem.201903014

WILEY-VCH

FULL PAPER

The Chiral Twist-Bend Nematic Phase (N^*_{TB})

Rebecca Walker[a]*, Damian Pociecha[b], John M.D. Storey[a], Ewa Gorecka[b] and Corrie T. Imrie[a]

Abstract: The twist-bend nematic, N_{TB}, phase has been observed for chiral material in which chirality is introduced through a branched 2-methylbutyl terminal tail. The chiral twist-bend nematic phase, N^*_{TB}, is completely miscible with the N_{TB} phase of the standard achiral material, CB6OCB. The N^*_{TB} phase exhibits optical textures with lower birefringence than those observed for the achiral N_{TB} phase, suggesting an additional mechanism of averaging molecular orientations. The N^*- N^*_{TB} transition temperatures for the chiral materials are higher than the N_{TB}-N transition temperatures seen for the corresponding racemic materials. This suggests the double degeneracy of helical twist sense in the N^*_{TB} phase is removed by the intrinsic molecular chirality. A square lattice pattern is observed in the N* phase over a temperature range of several degrees above N^*_{TB} – N phase transition, which may be attributed to a non-monotonic dependence of bend elastic constant.

Introduction

The spontaneous emergence of chirality in systems composed of achiral molecules is of fundamental importance in both physical and biological sciences and thought to play a pivotal role in the origin of biological homochirality. In this context the study of liquid crystalline systems has greatly enhanced our understanding of symmetry breaking in fluids [1]. Indeed, the first example of spontaneous chiral symmetry breaking in a fluid with no spatial ordering was provided by the twist-bend nematic, N_{TB}, phase in which the director forms a conical helix [2]. The formation of chirality in the N_{TB} phase is spontaneous and hence equal numbers of degenerate helices of opposite handedness would be expected. The pitch length in the N_{TB} phase is typically around 10 nm, just a few molecular lengths. Some 35 years before its experimental discovery, Meyer predicted the existence of the N_{TB} phase accounting for the director modulation in terms of flexoelectric couplings [3]. Later and independently, Dozov also predicted its existence within a framework in which the spontaneous director modulation arose from an elastic instability equivalent to a sign change of the bend elastic constant (K_{33}) [4].

[a] Dr. R. Walker, Prof. J.M.D Storey, Prof. C.T. Imrie
Department of Chemistry, School of Natural and Computing Sciences, University of Aberdeen
Meston Building, Aberdeen AB24 3UE (UK)
E-mail: rebecca.walker@abdn.ac.uk
[b] Dr. D. Pociecha, Prof. E. Gorecka
Faculty of Chemistry, University of Warsaw
ul. Zwirki i Wigury 101, 02-089 Warsaw (Poland)

Bent molecules are required to achieve low values of K_{33} [5] and hence, the overwhelming majority of twist-bend nematogens are odd-membered liquid crystal dimers - molecules containing two mesogenic units linked *via* a flexible alkyl spacer containing an odd number of atoms (for recent examples, see [6]). Dozov also predicted that achiral bent molecules should exhibit heliconical smectic phases [4] and these have recently been discovered [7].

The N_{TB} phase may be considered the generalised case of the chiral nematic phase, N*, the director of which is orthogonal to the helical axis. The N* phase is exhibited by chiral molecules and the molecular chirality provides the driving force for the formation of the helical structure. The pitch length of the N* phase is typically several hundred nanometres, some two orders of magnitude larger than that found in the N_{TB} phase.

The intriguing question now arises as to how the N_{TB} phase having spontaneous structural chirality will respond at a microscopic level to the presence of intrinsic molecular chirality. To investigate this, Meyer extended the elastic-instability model of the N_{TB} phase to consider the effect of a twist or chiral field introduced by chiral doping [8]. Within the framework of the model, the double degeneracy of the heliconical structure is removed and the ground state of the N_{TB} phase is predicted to have the same handedness as the dopant. The conical angle of the favoured heliconical state increases whereas the effect on the pitch is negligible. By comparison, the stability of the state having the opposite handedness decreases but remains metastable up to some given level of doping at which the degeneracy is completely removed. The pitch of the unfavoured helical state is essentially unchanged whereas the conical angle decreases on increasing doping concentration, vanishing when the state becomes unstable. Thus, chiral doping is predicted to increase the stability of the N_{TB} phase [8]. Longa and Tomczyk studied the effects of molecular chirality on the N_{TB} phase using minimum coupling Landau-de Gennes theory revealing the possibility of a polar, chiral twist-bend nematic phase [9].

There are two approaches to introduce molecular chirality into the N_{TB} phase, either by the addition of a chiral dopant or by the preparation of a chiral nematogen. The addition of a chiral dopant weakly destabilises the N_{TB} relative to the N phase and the removal of the degeneracy of the two heliconical states is observed [10]. Furthermore, doping the N_{TB} phase with a high helical twisting power (HTP) chiral dopant induces a lower temperature nematic phase suggested to be a variant of the N_{TB} phase and this is not observed for mixtures including low HTP dopants [10b, 11]. The N* phase shown by these doped twist-bend nematogens forms a conventional helical structure but the spontaneous formation of striped textures is observed a few degrees above the N^*-N^*_{TB} transition [12] attributed to K_{33} being smaller than the twist elastic constant, K_{22} [2b, 12b]. Above a given electrical or magnetic field, a heliconical state develops, the pitch of which may be tuned electrically or magnetically to give selective reflection of light ranging from the UV to infrared [13]. Most recently

Accepted Manuscript

This article is protected by copyright. All rights reserved.

it has been suggested, based on texture observations, that doping with a chiral dopant above a critical concentration induces a twist grain boundary (TGB) phase between the N* and N^*_{TB} phases [14].

Intrinsically chiral twist bend nematogens are extremely rare, and restricted to cholesteryl-based materials [15]. It was shown for these materials that the N^*_{TB} phase was miscible across the complete compositional range with the N_{TB} phase of the extensively studied CB7CB [15b] implying that the two phases are thermodynamically the same. However, the N_{TB}-N line on the phase diagram shows a negative curvature rather than positive as might be expected from Meyer's elastic-instability model [8]. This may result from a specific interaction between the differing mesogenic cores not accounted for in the model and such a view is supported by the negative curvature seen also for the N-I line [16]. The periodicity in the N^*_{TB} phase seen for the cholesteryl-based materials is about 11 nm and essentially identical to that observed in the N_{TB} phase of other materials [17]. Unfortunately, for these materials we do not have the corresponding achiral system to make a direct comparison of their properties.

It is clear that our understanding of the fundamentally important competition between spontaneous structural chirality and intrinsic molecular chirality is at a very early stage and here we report the first examples of chiral twist-bend nematogens along with their corresponding achiral counterparts. The simplest way to make a molecule chiral is to introduce an asymmetric carbon atom, acting as a chiral centre. In liquid crystalline systems this is often achieved by the addition of a methyl branch to a carbon atom in a terminal chain. It has been reported, however, that such a substitution strongly destabilises the N_{TB} phase,[18] presumably by disrupting the ability of the dimers to pack into an intercalated arrangement. Our design strategy was therefore to develop a high temperature twist-bend nematogen by the addition of a phenyl benzoate fragment to 4-butoxyphenyl 4-{[6-(4'-cyano[1,1'-biphenyl]-4-yl)hexyl]oxy}benzoate [18b] to which we could add a methyl branch without the loss of the N_{TB} phase. Thus, here we report the transitional properties of the 4-{[4-(alkyloxy)benzoyl]oxy}phenyl 4-[ω-(4'-cyano[1,1'-biphenyl]-4-yl)alkoxy]benzoates (Figure 1) and refer to them by the acronym CB*n*OPEPƎPO*m*, where CB denotes cyanobiphenyl, *n* the number of methylene units in the spacer, P a phenyl ring, E and Ǝ ester linkages in opposite directions, and m the nature of the terminal chain: *m*=4 denotes an n-butyl chain, *m*=(2-Me)4 a racemic 2-methylbutyl fragment, and *m*=(S)-(2-Me)4 a chiral 2-methylbutyl chain.

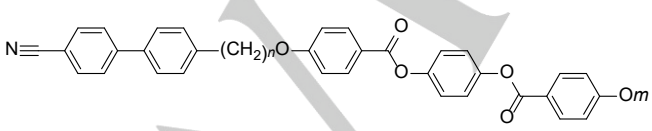

Figure 1. General structure of the CB*n*OPEPƎPO*m* dimers.

Results and Discussion

The transition temperatures and associated entropy changes for the CB*n*OPEPƎPO*m* dimers are listed in *Table 1*. All ten dimers exhibit either an enantiotropic nematic (N) or chiral nematic (N*) phase. These were identified on the basis of the observation of characteristic textures when viewed through the polarised light microscope (POM). Specifically, for the N phase a schlieren texture with two- and four- brush point defects, which flashes on the application of mechanical stress, was observed and for the N* phase an oily streak texture was seen. The values of the entropy changes associated with these transitions are wholly consistent with the phase assignments [19].

Table 1. Transition temperatures and associated entropy changes (in parentheses, scaled by R) for the CB*n*OPEPƎPO*m* dimers.

m	n	m.p.	SmA	N_{TB} / N^*_{TB}	N_{TB} / N^*_{TB}	I
4	**4**	154 (11.89)			• 249 (0.32)	•
4	**6**	154 (14.47)		• 95 (~0)	• 248 (0.54)	•
4	**8**	144 (15.44)		• 93[a]	• 241 (0.65)	•
4	**10**	135 (16.17)		• 90[a]	• 231 (0.72)	•
(S)-(2-Me)4	**4**	162 (15.56)			• 209 (0.23)	•
(S)-(2-Me)4	**6**	153 (15.27)		• 89[a]	• 214(0.33)	•
(S)-(2-Me)4	**8**	132 (16.23)		• 93[a]	• 212 (0.45)	•
(S)-(2-Me)4	**10**	131 (17.43)	• 88[a]		• 203 (0.58)	•
(2-Me)4	**6**	153 (17.67)		85[a]	• 214 (0.33)	•
(2-Me)4	**8**	131 (14.31)		92[a]	• 207 (0.38)	•

[a] Transition temperature obtained from microscopic observations.

On cooling the nematic phase for the CBnOPEPƎPO4 dimers with n = 6, 8 and 10, a monotropic twist-bend nematic (N_{TB}) phase formed. In a planar aligned cell the uniform texture of the N phase changed to give a striped texture characteristic of the N_{TB} phase (Figure 2), and the characteristic Brownian motion of the N phase ceased. The N–N_{TB} phase transition of CB6OPEPƎPO4 was evident using DSC as a small jump in the heat capacity (Figure 2) and this is in accord with the general observation that, as the temperature range of the preceding nematic phase increases, the N–N_{TB} transition tends towards becoming second order in nature [20].

To confirm phase assignment, binary mixtures of CB6OPEPƎPO4 with the extensively studied twist-bend nematogen CB6OCB [21] were used to construct a phase diagram (Figure 3). Continuous miscibility across the whole composition range confirms the assignments of the N_{TB} and N phases of CB6OPEPƎPO4. The N_{TB} phase of the binary mixtures did not readily crystallise and could be studied using X-ray diffraction (Figure 4). The patterns of the N and N_{TB} phases are essentially identical containing diffuse rings in both the small and wide-angle regions. The absence of layer reflections in the lower-temperature phase supports the assignment of the N_{TB} phase. The faint small-angle signals appear at approximately half the molecular length, suggesting a locally intercalated structure in both nematic phases.

Accepted Manuscript

This article is protected by copyright. All rights reserved.

10.1002/chem.201903014

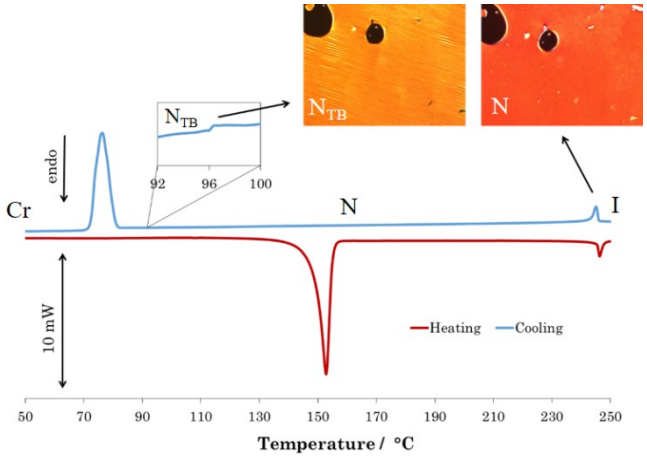

Figure 2. DSC heating and cooling traces for CB6OPEP∃PO4, with POM textures obtained in the nematic (108 °C) and twist-bend nematic (76 °C) phases in a 1.6 micron planar-aligned cell.

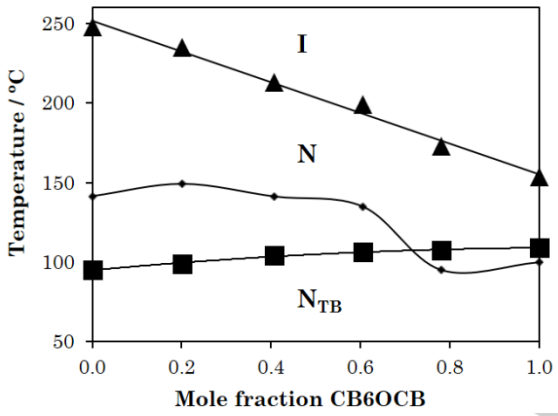

Figure 3. Phase diagram for CB6OPEP∃PO4/CB6OCB binary mixtures, where ▲ represents T_{NI}, ■ $T_{N_{TB}N}$, and ◆ the melting point.

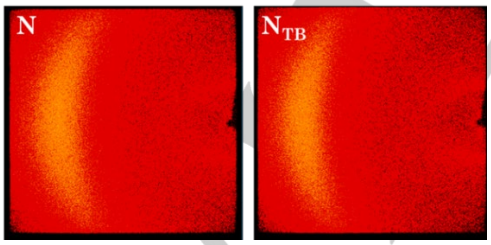

Figure 4. X-ray diffraction patterns obtained for 60 mol% CB6OPEP∃PO4/40 mol% CB6OCB in the nematic phase (left) and the twist-bend nematic phase (right).

Two CBnOPEP∃PO(2-Me)4 racemic dimers were prepared, *n*=6 and 8, to compare with the chiral dimers that exhibited the N^*_{TB} phase (see later). Both racemic dimers show a monotropic N_{TB} phase and an enantiotropic N phase assigned on the basis of textures as described earlier. It should be noted that this is the first observation of a N_{TB} phase for a compound with a branched terminal alkyl chain.The N_{TB} phase assignments were confirmed by the construction of binary phase diagrams with the twist-bend nematogen CB6OCB (Figure 5), and continuous miscibility of the components was observed across the whole composition range. Characteristic textures for the N and N_{TB} phases were seen for all the binary mixtures (Figure 6). Branching the terminal chain has reduced T_{NI} by 34 K for both dimers compared to the unbranched CB*n*OPEP∃PO4 analogues, with accompanying decreases in the entropy change associated with the N-I transition. These observations are indicative of an increase in local biaxiality in the N phase and decreased interaction strength parameter between the mesogenic units [22]. Interestingly, a much smaller reduction in $T_{N_{TB}N}$ is seen on chain branching, 10 K for *n*=6 and just 1K for *n*=8. This suggests that the interaction strength parameter between the mesogenic units plays a more critical role in determining T_{NI} than $T_{N_{TB}N}$. The similarity in $T_{N_{TB}N}$ for the *n*=8 dimers with linear and branched tails suggests that the difficulty associated with packing into an intercalated arrangement is relieved on increasing spacer length.

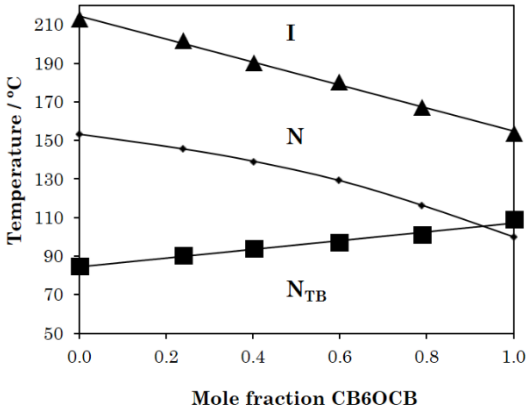

Figure 5. Phase diagram of the CB6OPEP∃PO(2-Me)4/CB6OCB binary mixture study, where ▲ represents T_{NI}, ■ $T_{N_{TB}N}$, and ◆ the melting point.

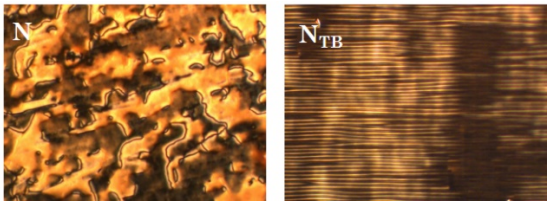

Figure 6. POM textures obtained for an 80:20 mol% mixture of CB6OPEP∃PO(2-Me)4:CB6OCB in the nematic (untreated slides, 179 °C) (left) and twist-bend nematic (right) phases (planar cell, 80 °C).

All the studied chiral dimers show an enantiotropic chiral nematic phase, N*, identified on the basis of the observation a of non-birefringent oily streak texture. For *n*=4 no other liquid crystalline phase is observed. For *n*=10, on cooling the N* phase a focal conic fan texture develops characteristic of a smectic A phase,

Accepted Manuscript

This article is protected by copyright. All rights reserved.

the assignment is confirmed by X-ray diffraction (Figure 7). Specifically, the diffuse small angle signal seen in the pattern of N* phase sharpens implying the formation of a lamellar phase whereas the wide angle reflection remains broad indicating liquid-like ordering within the layers. The ratio of the layer periodicity to the estimated all-*trans* molecular length is *ca* 0.5 and consistent with the formation of an intercalated smectic A phase.

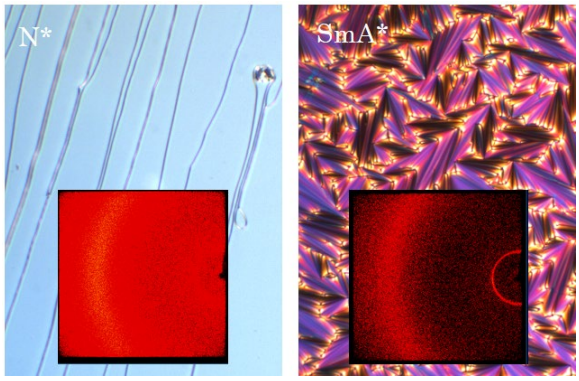

Figure 7. POM textures obtained for (S)-CB10OPEPƎPO(2-Me)4 in the chiral nematic phase at 116 °C (left) and the smectic A* phase at 85 °C (right), with corresponding X-ray diffraction patterns.

We will focus on the behaviour of the chiral dimers with n=6 and 8. None of them exhibited blue phases which is surprising given that similar odd-membered dimers have been shown to form blue phases whereas even members do not, and this difference was attributed to the lower twist elastic constants of the former [23]. On cooling, both chiral dimers easily crystallised, hindering the observation of any additional liquid crystalline phases in bulk samples. It was possible, however, to supercool isolated droplets of both to reveal a transition to a lower temperature liquid crystal phase. The unusual texture exhibited by these small droplets did not allow for the assignment of the phase. In thin cells treated for planar alignment, the material could be supercooled to reveal the lower temperature phase (Figure 8). At the transition from the N* phase to the lower temperature phase, the birefringence decreased much more strongly than in the case of the N-N_{TB} phase transition in achiral materials, and in addition the typical stripe pattern of N_{TB} was not formed. Instead a system of faint defect lines running in almost orthogonal directions were seen. Strong lowering of optical birefringence in N^*_{TB} phase suggests an additional mechanism of molecular orientation averaging, possibly by the twist in the direction perpendicular to the heliconical axis.

To establish whether this was the N^*_{TB} phase, a phase diagram of (S)-CB6OPEPƎPO(2-Me)4 and CB6OCB mixtures was constructed (Figure 9) and the complete miscibility observed over the complete compositional range confirmed the assignment. The N^*_{TB}-N transition temperatures are higher for the chiral dimers than seen for the racemic counterparts in accord with the predictions of the elastic instability model described by Meyer [8] although we note that these differences are small. It is interesting to note, however, that these small increases are also seen on comparing the transition temperatures for the mixtures of CBO6CB with the chiral and achiral analogues (Figures 5 and 9).

The monotropic nature of the N^*_{TB} phase shown by the chiral dimers precluded its detailed study but the mixtures with CB6OCB tended not to crystallise. The textures obtained for the N^*_{TB} phase of the mixture containing 60 mol % n=6 are shown in Figure 10. There are some similarities to the textures seen for the N_{TB} phase including regions of stripes but there are a number of different textures including chain-like patterns, jagged/deformed stripe patterns and a more uniform texture containing faint defect lines orthogonal to the developing stripe/chain pattern (Figure 10).

We stress that these textures grow isothermally and have no reason to invoke the existence of an additional phase. The ESI includes a video of the N^*_{TB}-N* phase transition. We suggest that the textural changes on cooling reflect the unwinding of the long helix of the N* phase and the formation of instantaneous short helices [24] as the transition to the N^*_{TB} phase is approached. The X-ray diffraction patterns for the N^*_{TB} and N* phases of this mixture are shown in Figure S2, and these are identical to those seen for achiral systems (Figure 4).

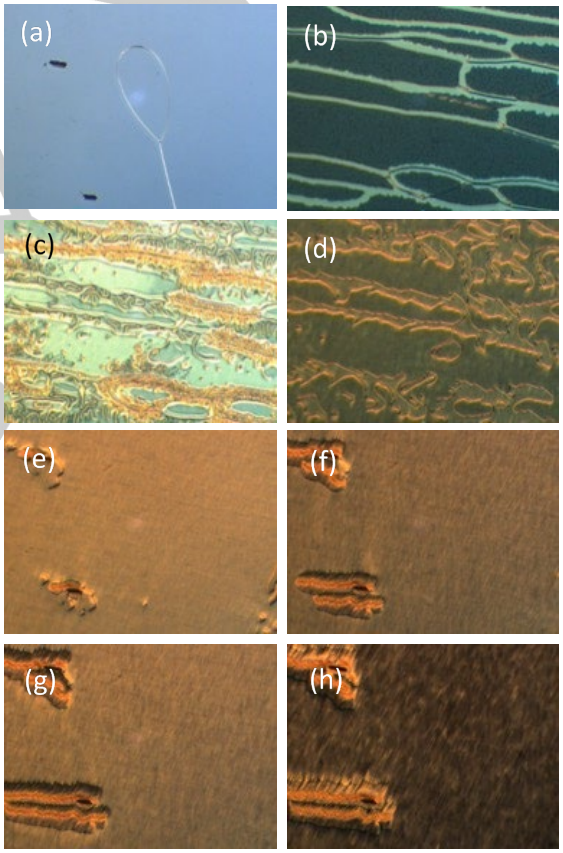

Figure 8. POM textures observed for (S)-CB8OPEPƎPO(2-Me)4. (a) Oily streak texture of the N* phase (100 °C); (b)-(d) N*-N*$_{TB}$ transition (~90 °C); (e)-(h) from the uniform texture of the N*$_{TB}$, isothermal development of jagged stripe pattern parallel to rubbing direction and faint defect lines orthogonal to the developing stripe/chain pattern.

Accepted Manuscript

This article is protected by copyright. All rights reserved.

10.1002/chem.201903014

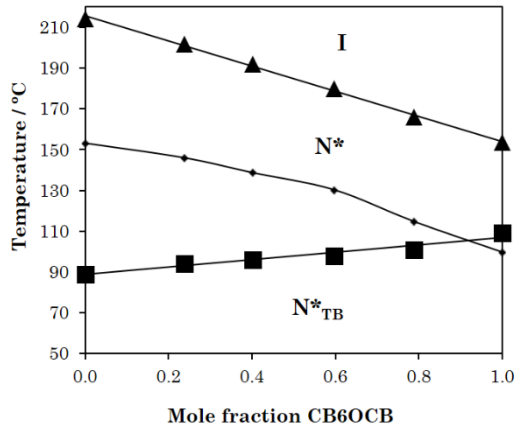

Figure 9. Phase diagram of the (S)-CB6OPEPƎPO(2-Me)4/CB6OCB binary mixture study, where ▲ represents T_{N^*I}, ■ $T_{N^*_{TB}N^*}$, and ◆ the melting point.

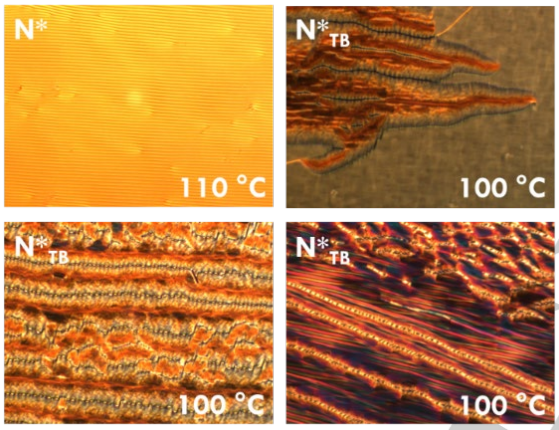

Figure 10. POM textures obtained for a 60:40 mol% mixture of (S)-CB6OPEPƎPO(2-Me)4:CB6OCB in the chiral twist-bend nematic phase.

A striking textural change is seen on cooling the N* phase in planar aligned cells for all the (S)-CB6OPEPƎPO(2-Me)4:CB6OCB mixtures and pure (S)-CB8OPEPƎPO(2-Me)4) prior to the formation of the N^*_{TB} phase, see Figure 11. Initially stripes develop perpendicular to the rubbing direction and these become crossed by perpendicular stripes to give a distinctive square lattice pattern. On further cooling the uniform texture of N* phase is restored. Similar behaviour has been reported recently by Salili *et al*. for chirally doped bent-core materials, and thought not to be associated with a thermodynamically distinct phase, but rather different modulated equilibrium director structures [12b]. Thus, in planar aligned cells, the helical axis of the N* phase is oriented perpendicular to the substrate. The free energy of the system is minimised when the cell thickness, *d*, is a multiple of the half pitch *p*/2. Since the pitch is temperature dependent, at most temperatures this condition is not fulfilled, and the helix becomes distorted. In a normal N* system the twist elastic constant is smaller than the bend, and so these deformations only involve twist. However, in the system studied here the bend elastic constant is smaller (or presumed to be smaller) and so we see different deformations now involving bend, resulting in this stripe and square textures. This pattern disappears consistently 10 K before the transition to the N^*_{TB} phase. The reason for this is not clear but may reflect the instantaneous formation of short pitch helices which influence the macroscopic bend elastic constant. A similar square grid pattern is sometimes observed in the SmC phase in the temperature range when the layer thickness changes abruptly, and has been explained as network of small parabolic domains.[25] While we cannot exclude such a reason as the origin of our observations, further experiments to explain this behaviour are now required.

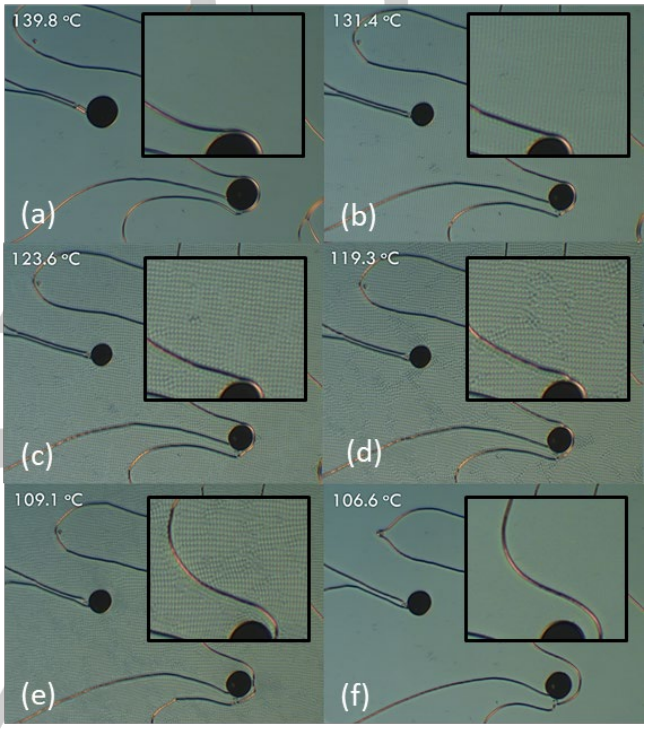

Figure 11. Development of the square lattice texture seen in 1.6 micron planar aligned cells above the $T_{N^*NTB^*}$ transition in CB6OPEPƎPO4*/CB6OCB 40/60 mol% mixture. (a) 139.8 °C, conventional oily streak texture of the N* phase (b) 131.4 °C, stripes perpendicular to rubbing direction (c) 123.6 °C, these are crossed by perpendicular stripes to give a square lattice pattern (d) 119.3 °C, further enhancement of the lattice pattern (e) 109.1 °C, lattice pattern begins to fade (f) 106.6 °C, approximately 10 °C above the N*-N^*_{TB} transition the pattern has completely vanished.

Conclusions

In summary, we have reported the synthesis and characterisation of new achiral compounds that exhibit the heliconical twist-bend nematic phase, N_{TB} and for the first time compare this behaviour with that observed for their chiral analogues. These chiral molecules exhibit the so-far rarely observed chiral twist-bend nematic phase, N^*_{TB}. The N^*_{TB}-N* transition temperatures are higher for the chiral dimers than seen for the racemic counterparts. This is in accord with theoretical predictions of the elastic instability model and suggests that the double degeneracy of helical twist sense in the N^*_{TB} phase is removed by the intrinsic

Accepted Manuscript

This article is protected by copyright. All rights reserved.

molecular chirality. The chiral and conventional forms of the N_{TB} phase are completely miscible, as for the N and N* phases.

Optically, these two phases exhibit strikingly different textures and studies are now required to establish the origins of these microscale differences.

Experimental Section

Materials All reagents and solvents available commercially were purchased from Sigma Aldrich, Alfa Aesar, ACROS Organics or TCI Chemicals and used as received.

Synthesis The synthesis of all reported dimers and their intermediates is described fully in the ESI.

Purity Analysis The proposed structures of all final products and their intermediates were characterised using a combination of ^{1}H and ^{13}C NMR, and FTIR spectroscopies. ^{1}H and ^{13}C NMR spectra were recorded on either a 400 MHz Varian Unity INOVA, or a 300 MHz Bruker Ultrashield NMR spectrometer. Infrared spectra were recorded on a Thermal Scientific Nicolet IR100 FTIR spectrometer with an ATR diamond cell. The purities of the final products were verified using C, H, N microanalysis performed by the Micro Analytical Laboratory in the School of Chemistry at the University of Manchester or Sheffield Analytical and Scientific Services Elemental Microanalysis Service at the University of Sheffield. These details are described fully in the ESI.

Enantiomeric Purity Analysis The enantiomeric purity of the dimers was determined through use of the chiral lanthanide shift reagent (CLSR) europium tris 3-(trifluoromethyl-hydroxymethylene)-(+)-camphorate, $Eu(tfc)_3$. These details are described in the ESI.

Polarised Optical Microscopy Phase characterisation was performed using polarised light microscopy using an Imager A2m polarizing microscope equipped with a Linkam heating stage. Glass cells were obtained from Warsaw Military University of Technology (WAT) having 1.6 or 3 micron thicknesses, and ITO conducting and 60 polymer aligning layers were used.

Differential Scanning Calorimetry The phase behaviour of the dimers was studied by differential scanning calorimetry using a Mettler-Toledo DSC1 fitted with an intracooler and calibrated using indium and zinc as standards. Heating and cooling rates were 10 ˚C min^{-1} and all samples were measured under a nitrogen atmosphere. Transition temperatures and associated enthalpy changes were extracted from the second heating trace unless otherwise noted. For each sample, two aliquots were measured and the data listed are the average of the two sets of data.

X-ray Diffraction Wide angle diffractograms (WAXS) were obtained with a Bruker D8 GADDS system (CuKα line, Goebel mirror, point beam collimator, Vantec2000 area detector). Samples were prepared as droplets on a heated surface.

Binary Mixture Studies Binary mixtures were prepared by co-dissolving pre-weighed amounts of each compound in dichloromethane or chloroform and allowing the solvent to evaporate slowly at room temperature. The mixtures were further dried in a vacuum oven at 50 °C for ~16 h.

Acknowledgements

EG and DP acknowledge the support of the National Science Centre (Poland): (Grant Number 2016/22/A/ST5/00319). RW gratefully acknowledges The Carnegie Trust for the Universities of Scotland for funding the award of a PhD scholarship.

Keywords: chirality • liquid crystals • spontaneous symmetry breaking • twist-bend nematic phase

[1] C. Tschierske, *Liq Cryst* **2018**, *45*, 2221-2252.

[2] (a) M. Cestari, S. Diez-Berart, D. A. Dunmur, A. Ferrarini, M. R. de la Fuente, D. J. B. Jackson, D. O. Lopez, G. R. Luckhurst, M. A. Perez-Jubindo, R. M. Richardson, J. Salud, B. A. Timimi, H. Zimmermann, *Phys Rev E* **2011**, *84*, 031704; (b) V. Borshch, Y. K. Kim, J. Xiang, M. Gao, A. Jakli, V. P. Panov, J. K. Vij, C. T. Imrie, M. G. Tamba, G. H. Mehl, O. D. Lavrentovich, *Nature Commun* **2013**, *4*, 2635; (c) C. H. Zhu, M. R. Tuchband, A. Young, M. Shuai, A. Scarbrough, D. M. Walba, J. E. Maclennan, C. Wang, A. Hexemer, N. A. Clark, *Phys Rev Lett* **2016**, *116*, 147803.

[3] R. B. Meyer, in *Molecular Fluids* (Eds.: R. Balian, W. G), Gordon and Breach, New York, **1976**.

[4] I. Dozov, *Europhys Lett* **2001**, *56*, 247-253.

[5] M. Cestari, E. Frezza, A. Ferrarini, G. R. Luckhurst, *Journal of Materials Chemistry* **2011**, *21*, 12303-12308.

[6] (a) R. J. Mandle, *Chemical Record* **2018**, *18*, 1341-1349; (b) D. A. Paterson, C. A. Crawford, D. Pociecha, R. Walker, J. M. D. Storey, E. Gorecka, C. T. Imrie, *Liquid Crystals* **2018**, *45*, 2341-2351; (c) E. E. Pocock, R. J. Mandle, J. W. Goodby, *Soft Matter* **2018**, *14*, 2508-2514; (d) R. Walker, D. Pociecha, J. P. Abberley, A. Martinez-Felipe, D. A. Paterson, E. Forsyth, G. B. Lawrence, P. A. Henderson, J. M. D. Storey, E. Gorecka, C. T. Imrie, *Chemical Communications* **2018**, *54*, 3383-3386; (e) A. Knezevic, I. Dokli, M. Sapunar, S. Segota, U. Baumeister, A. Lesac, *Beilstein Journal of Nanotechnology* **2018**, *9*, 1297-1307.

[7] (a) J. P. Abberley, R. Killah, R. Walker, J. M. D. Storey, C. T. Imrie, M. Salamonczyk, C. H. Zhu, E. Gorecka, D. Pociecha, *Nat Commun* **2018**, *9*, 228; (b) R. Walker, D. Pociecha, G. Strachan, J. M. D. Storey, E. Gorecka, C. T. Imrie, *Soft Matter* **2019**, *15*, 3188-3197; (c) M. Salamonczyk, N. Vaupotic, D. Pociecha, R. Walker, J. M. D. Storey, C. T. Imrie, C. Wang, C. H. Zhu, E. Gorecka, *Nat Commun* **2019**, *10*.

[8] C. Meyer, *Liq Cryst* **2016**, *43*, 2144-2162.

[9] L. Longa, W. Tomczyk, *Liq Cryst* **2018**, *45*, 2074-2085.

[10] (a) R. J. Mandle, E. J. Davis, C. T. Archbold, S. J. Cowling, J. W. Goodby, *J Mater Chem C* **2014**, *2*, 556-566; (b) C. T. Archbold, E. J. Davis, R. J. Mandle, S. J. Cowling, J. W. Goodby, *Soft Matter* **2015**, *11*, 7547-7557.

[11] R. J. Mandle, J. W. Goodby, *Soft Matter* **2018**, *14*, 8846-8852.

[12] (a) R. Balachandran, V. P. Panov, Y. P. Panarin, J. K. Vij, M. G. Tamba, G. H. Mehl, J. K. Song, *J Mater Chem C* **2014**, *2*, 8179-8184; (b) S. M. Salili, R. R. R. Almeida, P. K. Challa, S. N. Sprunt, J. T. Gleeson, A. Jaklia, *Liq Cryst* **2017**, *44*, 160-167.

[13] (a) J. Xiang, S. V. Shiyanovskii, C. T. Imrie, O. D. Lavrentovich, *Phys Rev Lett* **2014**, *112*; (b) J. Xiang, Y. N. Li, Q. Li, D. A. Paterson, J. M. D. Storey, C. T. Imrie, O. D. Lavrentovich, *Adv Mater* **2015**, *27*, 3014-3018; (c) S. M. Salili, J. Xiang, H. Wang, Q. Li, D. A. Paterson, J. M. D. Storey, C. T. Imrie, O. D. Lavrentovich, S. N. Sprunt, J. T. Gleeson, A. Jakli, *Phys Rev E* **2016**, *94*; (d) J. Xiang, A. Varanytsia, F. Minkowski, D. A. Paterson, J. M. D. Storey, C. T. Imrie, O. D. Lavrentovich, P. Palffy-Muhoray, *Proc Nat Acad Sci U S A* **2016**, *113*, 12925-12928.

[14] M. Murachver, A. Nemati, M. Salamonczyk, C. Bullock, Z. Sabata, V. Norman, C. Zhu, T. Hegmann, S. N. Sprunt, J. T. Gleeson, A. Jakli, *Soft Matter* **2019**, *15*, 3283-3290.

Accepted Manuscript

This article is protected by copyright. All rights reserved.

[15] (a) A. Zep, S. Aya, K. Aihara, K. Ema, D. Pociecha, K. Madrak, P. Bernatowicz, H. Takezoe, E. Gorecka, *J Mater Chem C* **2013**, *1*, 46-49; (b) E. Gorecka, N. Vaupotic, A. Zep, D. Pociecha, J. Yoshioka, J. Yamamoto, H. Takezoe, *Angew Chem Int Ed* **2015**, *54*, 10155-10159.

[16] R. Humphries, P. James, G. R. Luckhurst, *Symp. Faraday Soc.* **1971**, *5*, 107-118.

[17] M. Salamonczyk, N. Vaupotic, D. Pociecha, C. Wang, C. H. Zhu, E. Gorecka, *Soft Matter* **2017**, *13*, 6694-6699.

[18] (a) R. J. Mandle, E. J. Davis, C. T. Archbold, C. C. A. Voll, J. L. Andrews, S. J. Cowling, J. W. Goodby, *Chem: Euro J* **2015**, *21*, 8158-8167; (b) J. P. Abberley, S. M. Jansze, R. Walker, D. A. Paterson, P. A. Henderson, A. T. M. Marcelis, J. M. D. Storey, C. T. Imrie, *Liquid Crystals* **2017**, *44*, 68-83.

[19] (a) T. Donaldson, H. Staesche, Z. B. Lu, P. A. Henderson, M. F. Achard, C. T. Imrie, *Liq Cryst* **2010**, *37*, 1097-1110; (b) G. Y. Yeap, F. Osman, C. T. Imrie, *J Mol Struct* **2016**, *1111*, 118-125.

[20] D. A. Paterson, J. P. Abberley, W. T. Harrison, J. M. Storey, C. T. Imrie, *Liq Cryst* **2017**, *44*, 127-146.

[21] D. A. Paterson, M. Gao, Y. K. Kim, A. Jamali, K. L. Finley, B. Robles-Hernandez, S. Diez-Berart, J. Salud, M. R. de la Fuente, B. A. Timimi, H. Zimmermann, C. Greco, A. Ferrarini, J. M. D. Storey, D. O. Lopez, O. D. Lavrentovich, G. R. Luckhurst, C. T. Imrie, *Soft Matter* **2016**, *12*, 6827-6840.

[22] C. T. Imrie, *Liq Cryst* **1989**, *6*, 391-396.

[23] A. E. Blatch, I. D. Fletcher, G. R. Luckhurst, *J Mater Chem* **1997**, *7*, 9-17.

[24] D. Pociecha, C. A. Crawford, D. A. Paterson, J. M. D. Storey, C. T. Imrie, N. Vaupotic, E. Gorecka, *Phys Rev E* **2018**, *98*, 052706.

[25] C. S. Rosenblatt, R. Pindak, N. A. Clark and R. B. Meyer, *J Physique* **1977**, 38, 1105.

WILEY-VCH

Accepted Manuscript

This article is protected by copyright. All rights reserved.

10.1002/chem.201903014

WILEY-VCH

Entry for the Table of Contents (Please choose one layout)

FULL PAPER

New liquid crystal materials exhibiting the rarely observed chiral twist-bend nematic phase (N^*_{TB}) have been prepared and characterised. Their properties are compared to their racemic analogues, which exhibit conventional twist-bend nematic behaviour, and striking optical differences are observed.

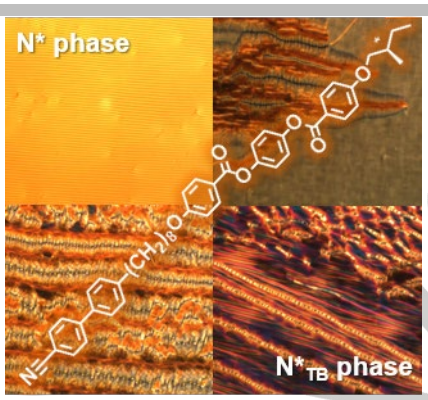

Rebecca Walker, Damian Pociecha, John M.D. Storey, Ewa Gorecka, Corrie T. Imrie.*

Page No. – Page No.

The Chiral Twist-Bend Nematic Phase (N^*_{TB})

WILEY-VCH

Accepted Manuscript

This article is protected by copyright. All rights reserved.